Neurobiology of Disease 106 (2017) 214–221

Contents lists available at ScienceDirect

Neurobiology of Disease

journal homepage: www.elsevier.com/locate/ynbdi

The brain-penetrant 5-HT$_7$ receptor agonist LP-211 reduces the sensory and affective components of neuropathic pain

Mirko Santello [a,c,d,*,1], Alberto Bisco [a,1], Natalie Elisabeth Nevian [a], Enza Lacivita [e], Marcello Leopoldo [e], Thomas Nevian [a,b,*]

[a] Department of Physiology, University of Bern, Bühlplatz 5, 3012 Bern, Switzerland
[b] Center for Cognition, Learning and Memory, University of Bern, Bern, Switzerland
[c] Institute of Pharmacology and Toxicology, University of Zürich, Winterthurerstrasse 190, 8057 Zürich, Switzerland
[d] Neuroscience Center Zurich, University of Zurich and ETH Zurich, 8057 Zurich, Switzerland
[e] Department of Pharmacy – Drug Science, University of Bari Aldo Moro, Via Orabona 4, 70125 Bari, Italy

ARTICLE INFO

Article history:
Received 22 February 2017
Revised 4 July 2017
Accepted 4 July 2017
Available online 6 July 2017

Keywords:
Neuropathic pain
Anterior cingulate cortex
HCN channels
Pyramidal neuron

ABSTRACT

Neuropathic pain is a debilitating pathological condition of high clinical relevance. Changes in neuronal excitability in the anterior cingulate cortex (ACC) play a central role in the negative emotional and affective aspects of chronic pain. We evaluated the effects of LP-211, a new serotonin-receptor-type-7 (5-HT$_7$R) agonist that crosses the blood-brain barrier, on ACC neurons in a mouse model of neuropathic pain. LP-211 reduced synaptic integration in layer 5 pyramidal neurons, which was enhanced in neuropathic pain due to a dysfunction of dendritic hyperpolarization-activated-and-cyclic-nucleotide-regulated (HCN) channels. Acute injection of LP-211 had an analgesic effect, increasing the mechanical withdrawal threshold in neuropathic animals, which was partially mediated by an action in the ACC. Additionally, the acute application of LP-211 blocked the switch in the place escape/avoidance behavior induced by noxious stimuli. Thus systemic treatment with a 5-HT$_7$R agonist leads to modulation of the ACC, which dampens sensory and affective aspects of chronic pain.

1. Introduction

The anterior cingulate cortex (ACC) is one of the key brain regions for the processing of pain (Basbaum et al., 2009; Devinsky et al., 1995; Zhuo, 2008). It is associated with encoding the emotional and aversive aspects of pain and it might be linked to the comorbid symptoms of chronic pain like depression (Barthas et al., 2015), lack of motivation (Navratilova and Porreca, 2014) and anxiety (Zhuo, 2016). Changes in the neuronal activity in this brain area are thought to be causally linked to the development of neuropathic pain (Baliki et al., 2012). Accordingly, hyperactivity has been observed in the human ACC in chronic pain states (Apkarian et al., 2009). On the cellular and network level a number of plastic changes induced by neuropathic pain have been described in the ACC ranging from increased cellular excitability and network restructuring (Blom et al., 2014) to malfunctioning synaptic plasticity mechanisms to promote hyperexcitability (Li et al., 2010). Recently we found that neuropathic pain causes a functional downregulation of hyperpolarization-activated-and-cyclic-nucleotide-regulated (HCN) channels in the dendrites of layer 5 (L5) pyramidal neurons in the ACC leading to cellular hyperexcitability due to enhanced dendritic integration of excitatory postsynaptic potentials (EPSPs) (Santello and Nevian, 2015). This malfunction of HCN channels in pyramidal neurons in the chronic pain condition was recently confirmed by a number of studies (Cordeiro Matos et al., 2015; Gao et al., 2016).

Therefore, targeting the ACC for a recovery of the pathologically enhanced neuronal activity might be a valid strategy to alleviate the emotional aspects of the neuropathic pain condition (Zhuo, 2008). Several pharmacological interventions or neuronal manipulations in the ACC have been proven effective in alleviating neuropathic pain behaviors (Gu et al., 2015; Li et al., 2010; Qu et al., 2011; Santello and Nevian, 2015). Particularly, approaches that utilize the brain's neuromodulatory systems might be a promising strategy for pain treatment without interfering with other essential signaling pathways in the brain (Santello and Nevian, 2015). Yet, a way to achieve neuromodulation in the ACC in behaving animals in a non-invasive manner is still lacking. We took advantage of the new brain penetrant 5-HT$_7$ receptor agonist LP-211 (Adriani et al., 2012; Hedlund et al., 2010; Leopoldo et al., 2008) to modulate neuronal activity and to evaluate its potential therapeutic effect on neuropathic pain behaviors.

* Corresponding authors at: Department of Physiology, University of Bern, Bühlplatz 5, 3012 Bern, Switzerland (T.N.) and Institute of Pharmacology and Toxicology, University of Zürich, Winterthurerstrasse 190, 8057 Zürich, Switzerland (M.S.).
E-mail addresses: mirko.santello@pharma.uzh.ch (M. Santello), nevian@pyl.unibe.ch (T. Nevian).
[1] These authors contributed equally.
Available online on ScienceDirect (www.sciencedirect.com).

http://dx.doi.org/10.1016/j.nbd.2017.07.005

2. Materials and methods

2.1. Neuropathic pain model

All the experiments were conducted after the approval of the Bern cantonal veterinary office (Switzerland). Only adult C57BL/6 male mice (8–12 weeks) were used. Mice were housed in groups of 5 in non-filtered cages, with a non-inverted 12 h day-night cycle and food/drink *ad libitum*. Mice were deeply anesthetized (Isoflurane) and then maintained with lower anesthesia concentration (1–1.5%) during the surgery. The surgeries were conducted under a sterile hood with laminar air flow. Temperature was maintained constant using an electric heating pad with rectal probe. The eyes were maintained humidified with the application of eye drops (Alcon, Switzerland). After the removal of the fur with a depilatory cream (Veet, Reckitt Benckiser, Switzerland), an incision on the left posterior thigh was made to allow the Chronic Constriction Injury of the exposed sciatic nerve through three loose ligations 1 mm apart (5-0 Sofsilk tread - US Surgicals). Animals whose nerve was exposed but left untouched were used as control group (sham). The wound was sutured using 4-0 coated VICRYL rapid suture (Ethicon). The animals recovered from the surgery after ~5 min and did not receive any postoperative analgesic treatment.

2.2. Von Frey test

The mechanical sensitization caused by CCI surgery was assessed using the electronic Von Frey filament test (IITC Life Science). To record the mechanical threshold the mice were habituated in a room at 20–23 °C with basal noise levels on a metal grid for ~30 min and then tested with the application of the Von Frey filament on the central plantar paw until the spontaneous retraction was detected. Six measures per each paw were averaged to verify the development of the mechanical hyperalgesia. CCI mice were tested at −4, −1, +3, +6 days from the surgery.

Von Frey testing was used to assess the modulation of the mechanical hypersensitivity by LP-211 treatment in the CCI pain model. In these experiments the animals were tested with the following time course: day −4, +7 relative to the surgery and +30, +60, +90, +120, +150, +180 min after the injection. When we performed the brain injection of SB-269970 together with i.p. injection of LP-211 or saline, the time course followed with the Von Frey testing was −4, +7 days relative to the surgery and +30, +45, +60, +90, +120 min from the end of the brain injection.

2.3. Acute brain slice preparation and patch-clamp electrophysiology

300 μm-thick coronal ACC brain slices were obtained from CCI or Sham mice 7 to 10 days after the surgery. Anesthetized animals were decapitated and the brain was quickly removed from the skull and maintained in ice-cold oxygenated (95% O_2 and 5% CO_2) slicing solution (65 mM NaCl, 2.5 mM KCl, 1.25 mM NaH_2PO_4, 25 mM $NaHCO_3$, 7 mM $MgCl_2$, 0.5 mM $CaCl_2$, 25 mM glucose, and 105 mM sucrose) for the slicing procedure. Brains were mounted on a vibratome (HM 650, Micron) inside a slicing chamber containing the same ice-cold solution. Slices were then transferred into aCSF solution (125 mM NaCl, 2.5 mM KCl, 1.25 mM NaH_2PO_4, 25 mM $NaHCO_3$, 1 mM $MgCl_2$, 2 mM $CaCl_2$, and 25 mM glucose) at 34 °C for 45 min and then at room temperature until use.

All the electrophysiological experiments were conducted on animals that were before tested with the electronic Von Frey filament and all the recordings were performed at 32–33 °C using aCSF as above. The recordings were conducted on rostroventral ACC pyramidal cell of the layer 5 (1.1–1.4 mm below the pial surface, 1.1–0.2 mm rostral to the Bregma and contralateral to the lesion) with a Leica DMLFS microscope (63× water-immersion objective), oblique illumination and CCD camera. The selection of the pyramidal cells to patch was based on their somatic morphology and on the presence of clearly visible thick apical dendrite. Recording pipettes with a thick borosilicate wall (resistance 5–9 MΩ) were used. The dendritic patch clamp, always performed near the main apical bifurcation, was achieved with 15–17 MΩ pipettes with the same intracellular solution (130 mM potassium gluconate, 5 mM KCl, 10 mM HEPES, 10 mM Na+-phosphocreatine, 4 mM Mg2+-ATP, 0.3 mM Na+-GTP, 0.2% biocytin (pH 7.3)). Biocytin was used to allow the cell reconstruction after PFA fixation (avidin-biotin-peroxidase method (Egger et al., 2008; Sieber et al., 2013)).

Data were acquired with a Dagan BCV-700A amplifier (Dagan Corporation, Minneapolis, MN, USA). Signals were digitized with an ITC-18 board (HEKA Electronics, Lambrecht, Germany). Electrode capacitance and series resistance was compensated at the beginning of the recording and regularly checked and readjusted. Voltage was filtered at 5 kHz and digitalized at 10 kHz. Focal electrical synaptic stimulation was achieved by placing a theta patch-pipette located in the inner layer 1, 30–80 μm lateral to the main apical dendrite. Stimulation intensity was manually adjusted (usually 1–3 V) to obtain a stable baseline (average amplitude 5.42 ± 0.58 mV). LP-211 was bath-applied at the concentration of 27 nM. After recording, pipettes were gently retracted and slices were placed in 4% paraformaldehyde (PFA). Slices were developed with the avidin-biotinperoxidase method and mounted on cover slides. Neurolucida reconstructions were performed to reveal the morphology of the cells. Axonal projections were omitted.

2.4. Immunohistochemistry and fluorescence imaging

5-HT_7 and HCN channels were co-stained to allow the visualization of the pattern of expression in the cortical layers of the ACC. Brain slices for fluorescent immunohistochemical double labeling were prepared from perfusion-fixed brains and staining procedures described by (Nolan et al., 2007; Santoro et al., 2009) were used. Animals were anesthetized with ketamine/xylazine and cardially perfused with PBS, followed by 4% PFA diluted in PBS. Fixed brains were removed and postfixed in 4% PFA at 4 °C overnight. After washing the brain with PBS (4 × 10 min), 50 um thick coronal brain slices were prepared and permeabilized in PBS containing 0.1% Triton-X100 (3 × 10 min). For double immunolabeling of HCN channels and $5HT_7$ receptors, slices were incubated for 1 h in a blocking buffer containing 5% normal chicken serum (NCS) and then simultaneously incubated in goat polyclonal anti-HCN1 (Santa Cruz, sc-19706; 1:250) and rabbit polyclonal anti-$5HT_7$ (Novus, NBP1-46598; 1:250) in NCS blocking buffer overnight. After primary incubation, slices were washed in PBS containing 0.1% Triton-X100 (3 × 10 min) and incubated in fluorescence conjugated secondary antisera (Alexa-594 chicken anti-goat IgG; Life Technologies, A21468; 1:500 and Alexa-488 chicken anti-rabbit IgG; Life Technologies, A21441; 1:100) in NCS blocking buffer at room temperature for 3 h. After further washing with PBS containing 0.1% Triton-X100 (1 × 10 min) and washing in PBS (3 × 10 min), slices were embedded in UltraCruz mounting medium on microscopy slides. Fluorescently labeled coronal brain slices were imaged using a confocal microscope (Leica SP8) equipped with a white-light laser and two GaAsP-detectors (HyD). Imaging was performed with a 20× objective (Leica, HC PL APO, 20×, NA 0.75 IMM CORR CS2) from the rostral ACC. In control experiments, slices were treated similarly, but the primary antibodies were omitted. No unspecific staining was observed in this case. Specificity of the 5-HT_7R antibody was further asserted by detecting no specific staining (*i.e.* of apical dendrites) in other selected brain areas.

2.5. In vivo drug testing

LP-211 was maintained in stock solution with ethanol and then used diluted in saline (NaCl 0.9%). SB-269970 was bilaterally injected in the brain (0.5 μl per injection site, 100 μM) in solution with Alexa-594 hydrazide (100 μM) and aCSF.

All the pharmacological *in-vivo* treatments were performed on CCI animals tested with the Von Frey electronic filaments 7–10 days after the CCI surgery to verify the development of the mechanical allodynia and to find the reference baseline for the comparison with the drug effect. i.p. injections were performed in lightly anesthetize mice (1% Isoflurane) to avoid any stress which could have an impact on the behavioral result. Brain injections were performed on isoflurane anesthetized animals (2%), which were head fixed to allow the incision of the scalp and the exposure of the skull. Two holes were drilled with a dental drill (Osada electronics, Tokyo, Japan) above the ACC (0.70 mm rostral and 0.35 mm lateral from Bregma,) or above the hindpaw S1 region (−0.70 mm caudal and 1.95 mm lateral from Bregma). A micromanipulator was used to position the micropipette in place and an air pressure system was used to control the injection speed. Injections were performed at 1.95 mm depth from the skull for the ACC and 1 mm depth for S1 respectively. Injection site was *post hoc* verified by brain clearing and light sheet imaging (Santello and Nevian, 2015).

In the LP-211 + SB-269970 experiments, the i.p. injection of LP-211 was done 20 min before the brain injection of SB-269970.

2.6. Place escape/avoidance paradigm

Experiments were conducted on CCI mice 7–8 days after surgery between 10 a.m. and 15 p.m. The temperature of the behavior room was between 20 and 23 °C with a basal noise level. Always the same experimenter alone tested the animals. A cold light lamp pointing at the ceiling of the room was used to diffusely illuminate the room. An open-air custom built two compartment box (40.5 × 29.5 × 25 cm^3) was used for the place escape/avoidance paradigm (PEAP) experiment. The box was positioned on a metal grid to allow for hind paw stimulation. One compartment had transparent walls and the other black walls. The two compartments were separated by a door of 7 × 7 cm allowing free movement of the mouse between the dark and light side. The illumination was set to 180 LUX intensity. Some experiments were conducted at lower light intensity (~10 LUX) but we observed no difference in the resulting data. Thus, the two groups were pooled together. The bottom of the chamber was illuminated with an IR lamp (46 × 66 cm^2) allowing high contrast recording of the position of the animal by an IR camera. For each experiment the mouse was gently put inside the light compartment and the recording session was immediately started (total of 40 min). The test consisted of 10 min recording of free exploration followed by 30 min of paw stimulation according to the chamber the animal was in. The hind paws were stimulated every 15 s with a Von Frey filament (number 12). The uninjured paw was stimulated in the light compartment and the injured paw was stimulated in the dark compartment. The entire course of the experiment was recorded and analyzed using EthoVision XT (Noldus). The time spent in each compartment was determined in bins of 10 min and expressed as percentage of the time spent in the light compartment. The PEAP test of animals injected with LP-211 was started 1 h 40 min after the injection of the drug in order to reach its peak effect during the behavioral test.

2.7. Brain clearing

Isoflurane anesthetized mice were decapitated and the extracted brain was briefly washed in PBS and post-fixed in PFA 4% for 2 days at 4 °C. After 3 washings of 10 min in PBS, we applied the dehydration protocol with series of 30%, 50%, 70%, 80%, 95% and twice 100% EtOH washes. The brains were then processed for the clearing treatment and 3D–ultramicroscopy imaging using a LaVision Lightsheet microscope (Santello and Nevian, 2015).

2.8. Data analysis

Electrophysiological recordings were acquired with IgorPro (Wavemetrics) and analyzed with custom written Igor procedures.

The *sag* ratio was calculated with the equation sag ratio = ($V_{baseline}$ − V_{min}) / ($V_{baseline}$ − $V_{steady\text{-}state}$) where $V_{baseline}$ is the resting membrane potential, V_{min} is the minimum voltage reached soon after the hyperpolarizing current pulse and $V_{steady\text{-}state}$ is the voltage recorded a few milliseconds before the end of the stimulus. For simplicity, V_{max} refers to $V_{baseline}$ − V_{min} and V_{SS} (steady-state) refers to $V_{baseline}$ − $V_{steady\text{-}state}$ in the figures.

EPSP amplitude and integral and coefficient of variation (CV^2) were evaluated by averaging 10 seeps before and at least 15 min after LP-211 bath application (inter-stimulus interval 10 s). Paired-pulse ratio was calculated by averaging 4 sweeps (inter-stimulus interval 20 s). The inverse of the square CV was calculated by $1/CV^2 = m^2/\sigma^2$, with m being the average EPSP amplitude and σ the SD.

The antihyperalgesic drug effect was quantified from the ratio of the left to right hind paw withdrawal thresholds as follows: (E_t − $E_{predrug}$) / $E_{predrug}$ with E_t being the average ratio of the time points around the maximal antihyperalgesic effect. In particular, for the I.P. injection of LP-211 the 2 h timepoint was considered and for the I.P. injection of LP-211 + SB/Saline in the ACC and S1 the average between 30 and 45 min was considered.

Acquisition of the PEAP experiments was performed with Noldus EthoVision XT software. A speed threshold (2.5 cm/s) was applied to the last 10 min average of each acquisition session to verify that the animal had not been affected by the manipulation.

Statistical analysis was performed in Excel (Microsoft) and Prism (Graphpad) using paired or unpaired Student's *t*-test and or one-way RM-ANOVA for *in vivo* drug injections. Statistical significance was assumed for $p < 0.05$. Error bars represent the standard error of the mean (SEM).

2.9. Chemicals and solutions used

LP-211 (*N*-(4-cyanophenylmethyl)-4-(2-diphenyl)-1-piperazine hexanamide) was synthetized at the Department of Pharmacy, University of Bari "A. Moro" Bari, Italy and used for the *in-vivo* experiments at a concentration of 10 mg/kg and for patch-clamp experiments at 27 nM. A subset of PEAP experiments were conducted with 2.5 mg/kg LP-211 injection but the results did not differ from the 10 mg/kg concentration so they were pulled together for the statistical analysis. For the brain injection, the serotonin receptor antagonist (2R)-1-((3-Hydroxyphenyl)sulfonyl)-2-(2-(4-methyl-1-piperidinyl)ethyl) pyrrolidine hydrochloride (SB-269970, Sigma) was used at 100 μM. Alexa-594 hydrazide was obtained from Life Technologies (A-10438). All the chemicals for the electrophysiology solutions were obtained from Tocris.

3. Results

3.1. The brain-penetrant 5-HT_7R agonist LP-211 modulates dendritic HCN channels in ACC neurons

HCN channels are highly enriched in the apical dendrites on layer 5 (L5) pyramidal cells throughout the neocortex and they are subjected to modulation by activation of several G protein coupled receptors (He et al., 2014; Postea and Biel, 2011). We have recently identified a specific receptor, the serotonin type 7 receptor (5-HT_7R), which enhances dendritic HCN channel function of L5 pyramidal neurons in the ACC by elevating cAMP levels (Santello and Nevian, 2015). Immunohistochemical labeling of 5-HT_7R and HCN1 revealed a co-localization in the apical dendrites of L5 pyramidal cells in the ACC (Fig. 1A, B), pointing to a functional coupling between 5-HT_7R activation and HCN channel modulation. Neuropathic pain caused by chronic constriction injury (CCI) of the left sciatic nerve results in a down regulation of HCN channels in the apical dendrites (Santello and Nevian, 2015). We investigated if this pathological change concomitantly influenced the distribution of 5-HT_7Rs. Within one week after the peripheral nerve ligation, CCI

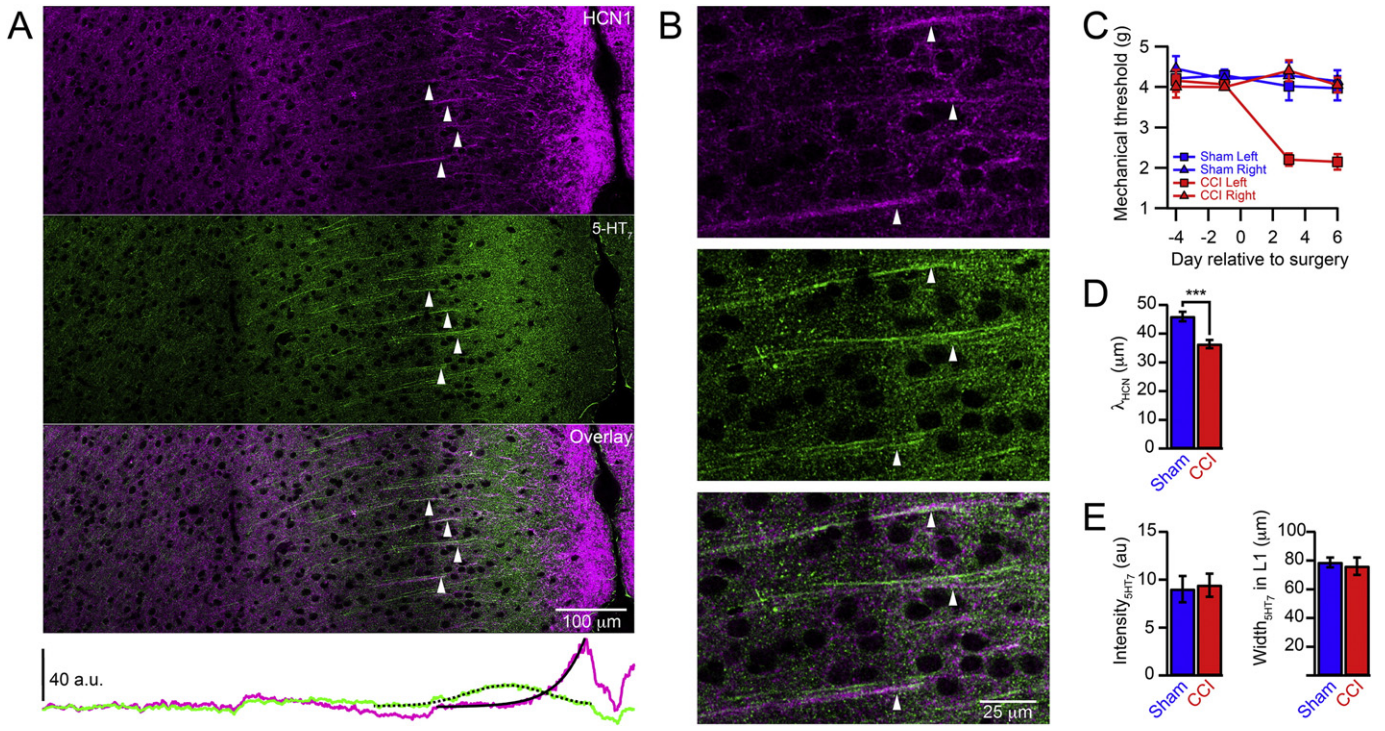

Fig. 1. 5-HT$_7$ receptors and HCN channels co-localize in apical dendrites. A. Immunohistochemical staining of HCN1 (magenta, top) and 5-HT$_7$Rs (green, middle) show a co-localization (white, bottom) of the two proteins in the main apical dendrites of L5 pyramidal cells (arrows) in the rostral ACC. The lower plot shows the intensity distribution for HCN1 and 5-HT$_7$Rs across the cortical layers. The solid black line represents a single exponential fit to the intensity profile of the HCN channel distribution. The dashed black line represents a Gaussian fit to the intensity profile of the 5-HT$_7$R distribution. B. Enlarged view of apical dendrites shown in (A). C. Mechanical paw withdrawal threshold of mice subjected to CCI of the left sciatic nerve (CCI, red; n = 7) and sham operated animals (Sham, blue; n = 6). Only the paw on the injured side displayed a reduction of the withdrawal threshold indicating mechanical hypersensitivity. D. Length constant λ_{HCN} of HCN1 distribution was significantly shorter for CCI as compared to sham operated animals. Error bars are S.E.M. ***p < 0.001. E. Fluorescence intensity and widths of 5-HT$_7$R distribution was not different for CCI and sham.

animals developed mechanical hypersensitivity restricted to the injured hind paw, which was not present in sham-operated mice (sham) (Fig. 1C). At this time point, we derived fluorescence intensity profiles from double immunohistochemical labeling of HCN channels and 5-HT$_7$Rs from brain slices of sham (n = 9 slices from 4 animals) and CCI (n = 9 slices from 4 animals) animals. HCN channel labeling showed a characteristic decrease from distal to proximal dendritic compartments, which was well fitted by a single exponential. The corresponding fluorescence length constant λ_{HCN} was significantly shorter in CCI as compared to sham animals (Fig. 1D, CCI 36.4 ± 1.4 µm, sham 46.0 ± 1.7 µm; $p < 0.001$) confirming our previous results (Santello and Nevian, 2015). 5-HT$_7$R labeling showed a Gaussian distribution in the distal apical dendrites with a peak in L2/3. The peak intensity and the width of this distribution were similar in CCI and sham (Fig. 1E, intensity: CCI 9.4 ± 1.2, sham 9.0 ± 1.4; $p = 0.83$; width: CCI 76.0 ± 6.1 µm, sham 78.7 ± 3.4 µm; $p = 0.74$) suggesting no apparent plasticity of 5-HT$_7$Rs.

In order to test now if the novel, brain-penetrant and highly selective 5-HT$_7$R agonist LP-211 has a similar modulatory effect on HCN channel function as previously shown with the less potent 5-HT$_7$R agonist 5-CT, we performed direct dendritic patch-clamp recordings in brain slices from the dendrites of L5 pyramidal neurons in the ACC of adult animals that had been subjected to CCI. Bath application of LP-211 induced a significant depolarization of the dendritic membrane potential (baseline −66.16 ± 1.33 mV; LP-211 −64.96 ± 1.21 mV, n = 5; $p < 0.05$). In parallel, the voltage *sag* in response to a hyperpolarizing current step increased (baseline 1.37 ± 0.07, LP-211 1.5 ± 0.08, n = 5; $p < 0.05$), indicating an enhancement of HCN channel function (Fig. 2A–C). Importantly, LP-211 had no influence on synaptic function, *i.e.* no influence on the amplitude or coefficient of variation of evoked EPSPs (Fig. 2D, E, amplitude: baseline 5.42 ± 0.57 mV, LP-211 5.26 ± 0.56 mV; CV^2: baseline 29.59 ± 1.14, LP-211 22.67 ± 4.06, n = 10; $p > 0.05$), suggesting no modulation of pre- and post-synaptic function by 5-HT$_7$Rs. Instead, we noticed a reduction in the single EPSP integral (baseline 143 ± 16 ms·mV, LP-211128 ± 16 ms·mV, n = 10; $p < 0.05$) as well as a reduction in EPSP summation, evaluated from the paired-pulse ratio of two EPSPs evoked at 50 Hz (Fig. 2F, second/first amplitude: baseline 2.10 ± 1.0, LP-211 1.73 ± 0.12, n = 10; $p < 0.05$). These results suggested that activation of 5-HT$_7$Rs by LP-211 lead to an increase in HCN channel function resulting in accelerated EPSP repolarization and a reduction in dendritic integration.

3.2. LP-211 is more effective in modulation of HCN channels than 5-CT

Bath application of LP-211 had a significant effect on the *sag* ratio measured with somatic whole-cell recordings (Fig. 3A, B). We found an increase in the somatic *sag* ratio in these experiments (baseline 1.26 ± 0.02, LP-211 1.31 ± 0.02, n = 18; $p < 0.05$) that was not observed with the 5-HT$_7$ agonist 5-CT (baseline 1.27 ± 0.02, 5-CT 1.24 ± 0.02, n = 10; $p = 0.08$). Indeed, there was a significant difference between LP-211 and 5-CT in modulating the somatic *sag* ratio (Fig. 3D, LP-211 1.04 ± 0.01, 5-CT 0.98 ± 0.01, $p < 0.001$). This suggests that LP-211 is more potent than 5-CT in modulating HCN channels. Furthermore, LP-211 increased the *sag* ratio in sham animals (Fig. 3E, Sham + LP-211 1.05 ± 0.02, $p < 0.05$) to a similar extend as in CCI animals ($p = 0.59$). Thus, the coupling of 5-HT$_7$Rs to HCN channels is independent from the pathological state.

3.3. Systemic injection of LP-211 reduces mechanical hypersensitivity and it partially acts by modulation of the ACC

Next, we tested if the reversal of the pathological condition that we observed on the cellular level by LP-211 *in vitro* had an influence on the pain behavior of neuropathic animals. LP-211 can readily cross the blood-brain-barrier and it has been shown to act in the central nervous

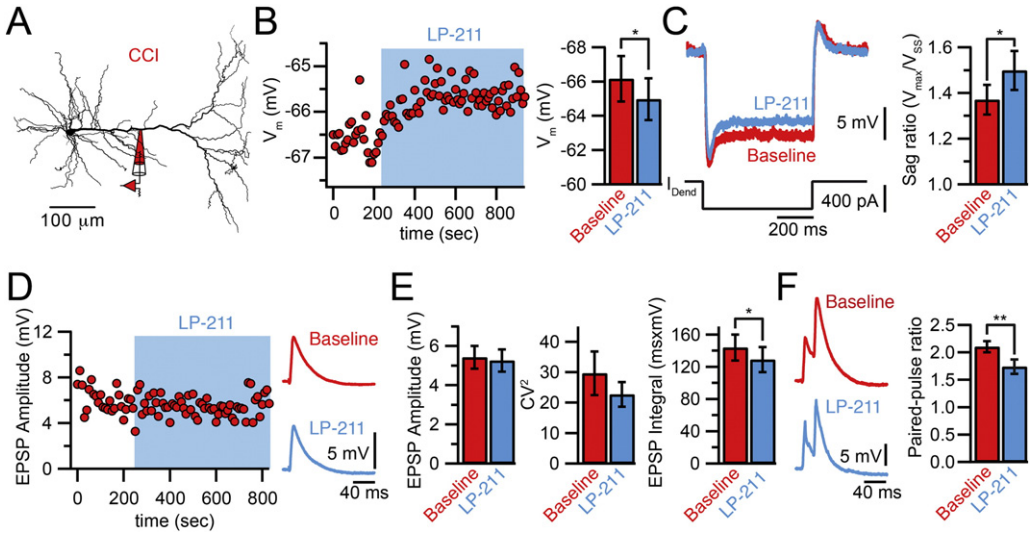

Fig. 2. Effect of 5-HT$_7$R activation by LP-211 on dendritic I_h and synaptic activity. A. Neurolucida reconstruction of a L5 pyramidal cell in the ACC showing the position of the dendritic recording pipette. All recordings in this figure were performed on slices from CCI animals. B. Time course of the dendritic resting membrane potential (V_m) during bath application of the 5-HT$_7$ agonist LP-211 (27 nM) from the cell shown in B. Summary bar graph shows average values. C. Example traces of the voltage response induced by a hyperpolarizing current step during baseline (red) and in the presence of LP-211 (blue) in a CCI animal. The average *sag* ratio showed a significant increase after bath application of LP-211 (n = 5). D. Time course of the EPSP amplitude during bath application of LP-211. Synaptic potentials were evoked by extracellular stimulation of the inner layer 1. Example traces show averaged EPSPs before and after the application of LP-211. E. EPSP amplitude and coefficient of variation (CV^2) were not affected by LP-211 whereas the EPSP time integral was reduced (n = 10). F. Paired EPSPs evoked at 50 Hz before and in presence of LP-211. Bar graph shows that the paired-pulse ratio was reduced by LP-211, indicating a reduction in temporal summation (n = 10). Error bars are SEM. *p < 0.05, **p < 0.01.

system (Leopoldo et al., 2008). Testing the effect of LP-211 on mechanical hypersensitivity induced by CCI, we found that a single i.p. injection increased the mechanical withdrawal threshold whereas saline injections had no effect (Fig. 4A–D). The analgesic drug response was effective after 30 min, reached a maximum between 90 and 150 min after injection and lasted at least 3 h. The maximal analgesic effect, expressed as the drug effect, was 0.58 ± 0.13 (n = 7) and significantly different from the saline injected controls (drug effect control: 0.04 ± 0.07, n = 6; p < 0.01).

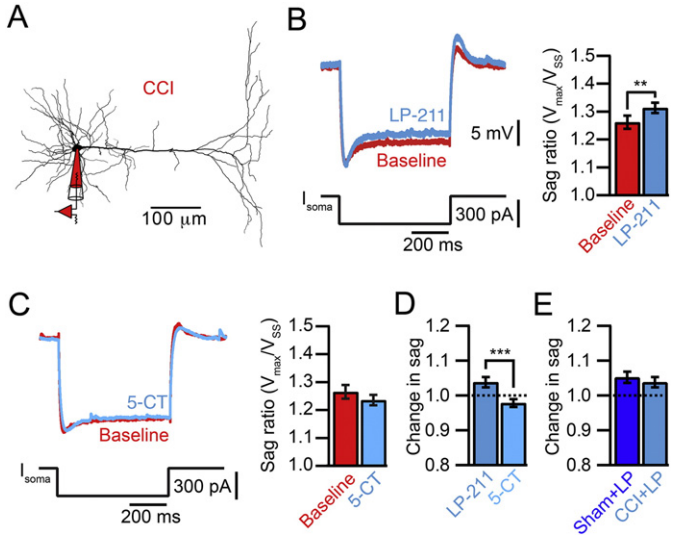

Fig. 3. LP-211 is more potent than 5-CT. A. Neurolucida reconstruction of a L5 pyramidal cell in the ACC showing the somatic recording configuration. All recordings in this figure were performed on slices from CCI animals. B. Somatic voltage response to a 300 pA hyperpolarizing current step before (red) and after bath application of LP-211. Bar graphs show an increase of the sag ratio by LP-211 (n = 18). C. Somatic voltage response before (red) and after bath application of 5-CT. Bar graphs show that 5-CT does not have an effect on the somatic sag ratio (n = 10). D. Normalized effect of LP-211 and 5-CT on the sag ratio. E. Normalized effect of LP-211 on the sag ratio in sham and CCI cells. Error bars are S.E.M. **p < 0.01 ***p < 0.001.

These results illustrate the potential therapeutic utility of LP-211 as an analgesic drug, which can be systemically injected. Nevertheless, the site of action has yet to be determined. Our findings that 5-HT$_7$ receptors are highly enriched in the dendrites of L5 pyramidal neurons in the ACC and that they co-localize and are functionally coupled with HCN channels suggest an involvement of cortical sites to its action. To determine the contribution of the ACC to the analgesic effect of systemic injection of LP-211, we inhibited 5-HT$_7$Rs specifically in the ACC by local injection of the selective antagonist SB-269970 together with systemic injection of LP-211 in CCI animals (Fig. 5). The block of 5-HT$_7$Rs in the ACC lead to a substantial reduction of the analgesic effect of LP-211 (Fig. 5C–E, drug effect, LP-211 + saline: 0.52 ± 0.08, n = 6; LP-211 +

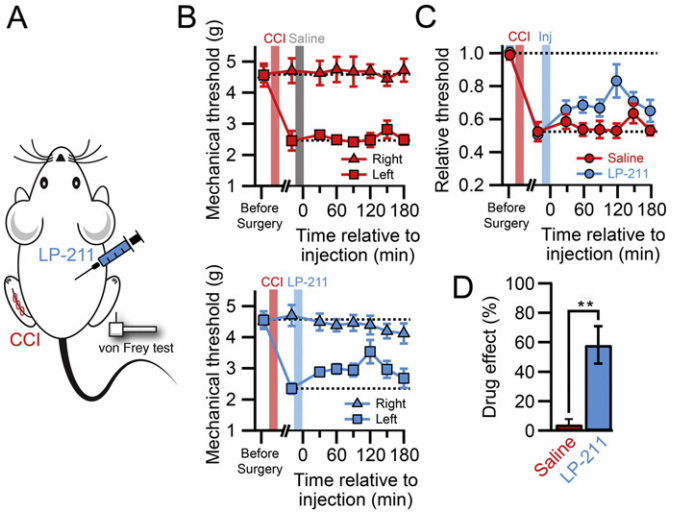

Fig. 4. Systemic LP-211 administration is analgesic for neuropathic pain. A. Experimental design for the i.p. injection of LP-211 or saline in CCI animals. B. Time course of the mechanical withdrawal threshold of mice subjected to CCI surgery and then tested after saline (upper graph, n = 6) or LP-211 injection (lower graph, n = 7). C. Withdrawal threshold of the injured paw normalized to the non-injured paw in saline (red) and LP-211 treated groups. D. Bar graph showing the drug effect of saline and LP-211 treated animals. Error bars are S.E.M. *p < 0.01.

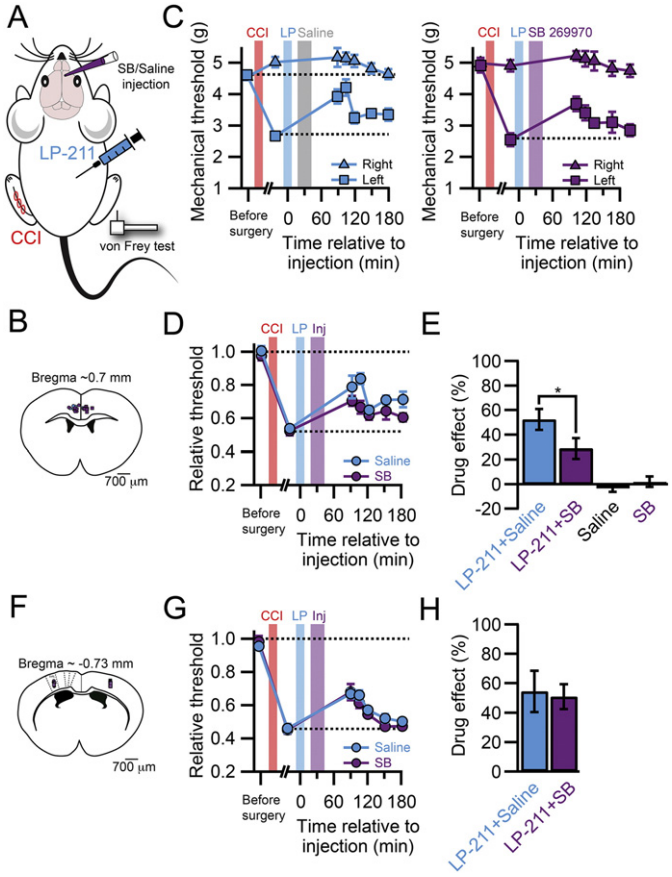

Fig. 5. Effect of 5-HT$_7$ antagonist injected in the ACC on LP-211 analgesia. A. Experimental design for the i.p. injection of LP-211 and concomitant cortical injection of SB-269970, or saline, in CCI animals and subsequent von Frey testing of mechanical sensitization. B. *Post hoc* localization of the injection sites in the ACC by Alexa594 co-injection, ex vivo clearing of the brain and reconstruction with 3D-ultramicroscopy. C. Time course of the mechanical withdrawal threshold of mice subjected to CCI surgery and treated with LP-211 after ACC injection of saline solution (upper graph, n = 6) or SB-269970 (lower graph, n = 6). At time t = −60 min LP-211 was i.p. injected and at t = −45 min the saline or SB269970 solution was injected. D. Withdrawal threshold of the injured paw normalized to the non-injured paw after LP-211 injection and subsequent injection of saline (blue) or SB-269970 (purple) in the ACC. E. Bar graph showing the drug effect of LP-211 treated animals after ACC injection of saline or SB-269970 showing a significant effect of 5-HT$_7$R blockade in the ACC on mechanical sensitization. Saline (n = 4) or SB-269970 (n = 7) injection into the ACC without LP-211 had no analgesic effect by itself. Error bars are S.E.M. *p < 0.05. F. *Post hoc* localization of the injection sites in S1 by Alexa594 co-injection, *ex vivo* clearing of the brain and reconstruction with 3D-ultramicroscopy. G. Withdrawal threshold of the injured paw normalized to the non-injured paw after LP-211 injection and subsequent injection of saline (blue) or SB-269970 (purple) in S1. H. Bar graph showing the drug effect of LP-211 treated animals after S1 injection of saline or SB-269970 showing no effect of 5-HT$_7$R blockade in the S1 on mechanical sensitization. Saline (n = 7) or SB-269970 (n = 8).

SB269970: 0.29 ± 0.08, n = 6; p < 0.05). Because local injections of SB-269970 *per se* did not reduce mechanical hypersensitivity (Fig. 5E, drug effect, saline: −0.03 ± 0.03 n = 4; SB-269970: 0.02 ± 0.04 n = 7), we concluded that LP-211 directly activated 5-HT$_7$ receptors in the ACC reducing the response to mechanical stimulation of the injured hind paw.

As a control for the specificity of the blocking action of SB-269970 in the ACC, saline or SB-269970 was injected into the region of the hind paw representation in the primary somatosensory cortex (S1) after IP injection of LP-211 (Fig. 5F–H). S1 is another important area involved in pain processing and its modulation can influence pain behavior (Eto et al., 2011). In contrast to the effect on the ACC, injection of SB-269970 in S1 produced no change in the LP-211-induced reduction of mechanical hypersensitivity (drug effect, saline: 0.54 ± 0.14, n = 7; SB-269970: 0.51 ± 0.08, n = 8; p = 0.41).

In summary, these results confirmed that LP-211 crossed the blood-brain-barrier and that it exerted its effect partially in the ACC, but that it is not generally acting on cortical areas involved in pain processing as exemplified by the absence of modulation in S1. Modulation of other brain areas, for example the PAG or the raphe nuclei, as well as an influence on the spinal cord, may account for the residual analgesic effect of the drug.

3.4. LP-211 reverses the place escape/avoidance behavior in CCI animals

The ACC is essential for the processing of the emotional/affective component of pain (Basbaum et al., 2009; Costigan et al., 2009; King et al., 2009; Navratilova and Porreca, 2014). We therefore tested if LP-211 was also able to modulate the affective aspects associated with neuropathic pain by using the place escape/avoidance paradigm (PEAP) (Fig. 6). This task requires processing in the ACC and it assesses the averseness of neuropathic pain by exploiting the conflict between the desire to avoid pain *versus* the safety of a preferred dark location (LaBuda and Fuchs, 2000; LaGraize et al., 2004). Animals were free to avoid a noxious stimulus given to the injured hind paw in the dark compartment by moving to the light compartment, where the contralateral paw was mechanically stimulated. Touching the corresponding paw was repeated every 15 s. Since LP-211 reduced the mechanical withdrawal response as measured with the von-Frey test, we used a much more rigid filament (number 12) to clearly evoke a supra-threshold, nociceptive response in the injured, left hind paw. CCI animals injected i.p. with a saline solution showed a switch in the place preference from the dark to the light compartment (Fig. 6A, B). In contrast, CCI animals injected with LP-211 did not show this switch and they were not affected by the noxious stimulation in the dark compartment anymore (relative time in light compartment,

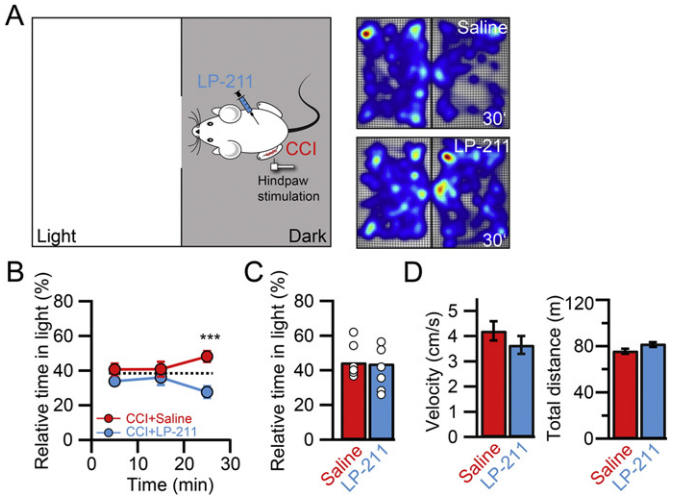

Fig. 6. LP-211 normalizes emotional pain behavior. A. Experimental design of the PEAP. The mouse can freely move between a light and dark compartment. The injured paw is stimulated in the dark compartment and the uninjured paw in the light compartment. Stimulation of the corresponding paw was repeated every 15 s. The heat maps on the right illustrate the time spent in each position 20–30 min after the beginning of the stimulation in a saline (top) and LP-211 (10 mg/kg, bottom) treated animal. In the saline treated condition, the animal spent less time in the preferred dark compartment. B. The relative time spent in the light compartment is plotted as a function of time. 20–30 min after the beginning of the stimulation of the corresponding hind paw, saline treated CCI animals showed a switch in place preference (red, n = 7). This switch was absent in LP-211 treated animals (blue, n = 8). The dashed line refers to the average of the first 10 min of the stimulation in the two conditions (37.3%). C. 10 min before the beginning of the stimulation the animals were allowed to freely explore the two compartments. The bar graph shows the relative time spent in the light compartment of saline and LP-211 treated animals. Open circles indicate individual experiments. LP-211 injection had no influence on the overall anxiety level. D. Average velocity and total distance covered of the animals during the recording period of 40 min. No differences were found for these parameters in saline and LP-211 treated animals. Error bars are S.E.M. *p < 0.05.

20–30 min after beginning of stimulation: saline: 48.2 ± 3.1%, n = 7; LP-211: 27.6 ± 3.4%, n = 8; $p < 0.05$). LP-211 had no effect on the spontaneous exploratory behavior evaluated within 10 min before the paws were stimulated (Fig. 6C; saline: 44.5 ± 3.7%; n = 7, LP-211: 43.9 ± 4.6%; n = 8; $p > 0.05$) ruling out general anxiolytic effects of LP-211 in this behavioral paradigm. Furthermore, LP-211 did not exert sedative effects on the animals since the average velocity (saline: 4.04 ± 0.38 cm/s; LP-211: 3.49 ± 0.37 cm/s; $p > 0.05$) and total distance covered (saline: 74.84 ± 1.25 m; LP-211: 77.44 ± 0.80 m; $p > 0.05$) were not affected (Fig. 6D). These results show that activation of 5-HT$_7$Rs by the blood-brain-barrier-penetrant specific agonist LP-211 can alleviate the emotional/affective pain behavior in mice experiencing neuropathic pain.

4. Discussion

On the cellular level chronic pain is established by persistent neuronal plasticity within the pain transmitting system (Basbaum et al., 2009; Costigan et al., 2009). Changes in cortical areas are of particular interest to understand the cognitive, motivational and emotional/affective aspects and deficits associated with the chronic pain condition (Apkarian et al., 2009; Simons et al., 2014).

We recently demonstrated that activation of 5-HT$_7$ receptors enhances HCN channel function and alleviates neuropathic pain, suggesting that neuromodulation in the forebrain might be a potential strategy for pain treatment. Here we studied the effects of LP-211, a highly specific 5-HT$_7$R agonist that penetrates the blood-brain barrier. The use of this compound allowed non-invasive treatment of animals with neuropathic pain by acute i.p. injections. Our results revealed for the first time that mechanical sensitization of the injured hind paw can be reduced by systemic treatment with LP-211 and that at least part of the action can be attributed to a mechanism modulating the ACC. In contrast, the primary somatosensory cortex, a brain area that is important for the localization of nociception, was not involved in the action of LP-211. This suggests that LP-211 is not globally dampening the activity of cortical areas involved in pain processing. Nevertheless, it has to be determined which other pain-related areas might also be contributing to the overall analgesic effect. 5-HT$_7$ receptors are expressed in the PAG and other brain areas as well as the spinal cord (Ciranna and Catania, 2014). Possible analgesic effects by activation of 5-HT$_7$Rs in these areas have previously been reported (Li et al., 2014; Lin et al., 2015). For instance, although activation of 5-HT$_7$Rs has no influence on acute pain behavior in naïve animals (Yesilyurt et al., 2015), an up regulation of 5-HT$_7$Rs in the dorsal horn of the spinal cord in neuropathic pain and a local analgesic effect of another 5-HT$_7$R agonist (E-57431) has been shown (Brenchat et al., 2010). In contrast, the immunohistochemical staining of 5-HT$_7$Rs in our case did not indicate such a plastic change in receptor expression in the ACC in the neuropathic pain condition. In general, activation of 5-HT$_7$Rs by descending serotoninergic pathways has been shown to be necessary for stress-induced analgesia. Moreover, the anti-hyperalgesic effects of morphine, of some antidepressants and non-opioid analgesic drugs also depend on 5-HT$_7$Rs (Dam et al., 2014; Dogrul and Seyrek, 2006), suggesting that these receptors might be the final target of some established pain treatments as well as of the endogenous pain regulatory systems.

LP-211 completely abolished the pain-induced shift in place preference in a place escape/avoidance paradigm. This behavioral assay depends on the ACC and it is thought to be related to the emotional/affective component of pain (LaBuda and Fuchs, 2000; LaGraize et al., 2004). This behavioral test assesses the averseness of neuropathic pain by exploiting the conflict between the desire to avoid pain *versus* the safety of an enclosed, dark location, which is usually preferred by the animal. Thus, we were able to show that LP-211 can reduce the emotional distress associated with chronic pain. Our results are consistent with previous findings reporting that LP-211 can modulate affective behavior and anxiety (Adriani et al., 2012) and extend these findings to the modulation of pain averseness.

In the ACC, we were able to determine the mechanism of action of LP-211 on the cellular level. 5-HT$_7$R activation increases HCN function *via* the stimulation of adenylate cyclase and an increase in cAMP levels as has been demonstrated previously (Chapin and Andrade, 2001; Santello and Nevian, 2015; Tang and Trussell, 2015), resulting in decreased temporal summation of EPSPs and thus decreased cellular excitability of L5 pyramidal neurons. Importantly, we did not find any synaptic modulation suggesting that 5-HT$_7$Rs are not involved in synaptic transmission. Previously, we have shown that there is also no influence on inhibitory interneurons and L2/3 pyramidal neurons in the ACC (Santello and Nevian, 2015). Alternative pathways downstream of 5-HT$_7$R activation could be through protein kinase A (PKA) or other direct G-protein interactions (Perez-Garci et al., 2013). We have previously shown that the activation of 5-HT$_7$Rs has no further influence on cellular excitability when HCN channels are blocked, excluding an apparent alternative mode of action in L5 pyramidal neurons in the ACC (Santello and Nevian, 2015).

In light of a potential translational utility of LP-211, the specificity of activating a particular 5-HT receptor subtype that decreases neuronal excitability might be beneficial compared to increasing 5-HT levels in the brain globally with tricyclic antidepressants. Moreover, chronic LP-211 treatment may cause 5-HT$_7$Rs upregulation and therefore might cause persistent beneficial effects, as it has been shown in other pathological models (Nativio et al., 2015; Ruocco et al., 2014).

The 5-HT$_7$ receptor has been little studied so far, mainly due to the lack of a specific agonist. The development of new brain-penetrant and specific 5-HT$_7$Rs agonists is now helping shedding light on the pathophysiological role of this receptor, which has been documented to be present in several areas of the human nervous system including the anterior cingulate gyrus (Slassi et al., 2004). The results presented here together with the reported analgesic effects of activating 5-HT$_7$Rs in the spinal cord, point to a central role for this receptor in pain modulation and suggest a novel and specific treatment strategy for chronic pain that acts both on spinal and supra-spinal targets.

Acknowledgements

We thank Hanns-Ulrich Zeilhofer, Isabelle Decosterd and their groups for training in CCI surgery and behavioral testing. This work was supported by the Swiss National Science Foundation (T.N., grant PP00P3_128415 and 31003A_159872) and the European Research Council (T.N., grant 682905).

References

Adriani, W., Travaglini, D., Lacivita, E., Saso, L., Leopoldo, M., Laviola, G., 2012. Modulatory effects of two novel agonists for serotonin receptor 7 on emotion, motivation and circadian rhythm profiles in mice. Neuropharmacology 62, 833–842.

Apkarian, A.V., Baliki, M.N., Geha, P.Y., 2009. Towards a theory of chronic pain. Prog. Neurobiol. 87, 81–97.

Baliki, M.N., Petre, B., Torbey, S., Herrmann, K.M., Huang, L., Schnitzer, T.J., Fields, H.L., Apkarian, A.V., 2012. Corticostriatal functional connectivity predicts transition to chronic back pain. Nat. Neurosci. 15, 1117–1119.

Barthas, F., Sellmeijer, J., Hugel, S., Waltisperger, E., Barrot, M., Yalcin, I., 2015. The anterior cingulate cortex is a critical hub for pain-induced depression. Biol. Psychiatry 77, 236–245.

Basbaum, A.I., Bautista, D.M., Scherrer, G., Julius, D., 2009. Cellular and molecular mechanisms of pain. Cell 139, 267–284.

Blom, S.M., Pfister, J.P., Santello, M., Senn, W., Nevian, T., 2014. Nerve injury-induced neuropathic pain causes disinhibition of the anterior cingulate cortex. J. Neurosci. 34, 5754–5764.

Brenchat, A., Nadal, X., Romero, L., Ovalle, S., Muro, A., Sanchez-Arroyos, R., Portillo-Salido, E., Pujol, M., Montero, A., Codony, X., Burgueno, J., Zamanillo, D., Hamon, M., Maldonado, R., Vela, J.M., 2010. Pharmacological activation of 5-HT7 receptors reduces nerve injury-induced mechanical and thermal hypersensitivity. Pain 149, 483–494.

Chapin, E.M., Andrade, R., 2001. A 5-HT(7) receptor-mediated depolarization in the anterodorsal thalamus. II. Involvement of the hyperpolarization-activated current I(h). J. Pharmacol. Exp. Ther. 297, 403–409.

Ciranna, L., Catania, M.V., 2014. 5-HT7 receptors as modulators of neuronal excitability, synaptic transmission and plasticity: physiological role and possible implications in autism spectrum disorders. Front. Cell. Neurosci. 8, 250.

Cordeiro Matos, S., Zhang, Z., Seguela, P., 2015. Peripheral neuropathy induces HCN channel dysfunction in pyramidal neurons of the medial prefrontal cortex. J. Neurosci. 35, 13244–13256.
Costigan, M., Scholz, J., Woolf, C.J., 2009. Neuropathic pain: a maladaptive response of the nervous system to damage. Annu. Rev. Neurosci. 32, 1–32.
Dam, L.J., Hai, L., Ha, Y.M., 2014. Role of the 5-HT(7) receptor in the effects of intrathecal nefopam in neuropathic pain in rats. Neurosci. Lett. 566, 50–54.
Devinsky, O., Morrell, M.J., Vogt, B.A., 1995. Contributions of anterior cingulate cortex to behaviour. Brain 118 (Pt 1), 279–306.
Dogrul, A., Seyrek, M., 2006. Systemic morphine produce antinociception mediated by spinal 5-HT7, but not 5-HT1A and 5-HT2 receptors in the spinal cord. Br. J. Pharmacol. 149, 498–505.
Egger, V., Nevian, T., Bruno, R.M., 2008. Subcolumnar dendritic and axonal organization of spiny stellate and star pyramid neurons within a barrel in rat somatosensory cortex. Cereb. Cortex 18, 876–889.
Eto, K., Wake, H., Watanabe, M., Ishibashi, H., Noda, M., Yanagawa, Y., Nabekura, J., 2011. Inter-regional contribution of enhanced activity of the primary somatosensory cortex to the anterior cingulate cortex accelerates chronic pain behavior. J. Neurosci. 31, 7631–7636.
Gao, S.H., Wen, H.Z., Shen, L.L., Zhao, Y.D., Ruan, H.Z., 2016. Activation of mGluR1 contributes to neuronal hyperexcitability in the rat anterior cingulate cortex via inhibition of HCN channels. Neuropharmacology 105, 361–377.
Gu, L., Uhelski, M.L., Anand, S., Romero-Ortega, M., Kim, Y.T., Fuchs, P.N., Mohanty, S.K., 2015. Pain inhibition by optogenetic activation of specific anterior cingulate cortical neurons. PLoS One 10, e0117746.
He, C., Chen, F., Li, B., Hu, Z., 2014. Neurophysiology of HCN channels: from cellular functions to multiple regulations. Prog. Neurobiol. 112, 1–23.
Hedlund, P.B., Leopoldo, M., Caccia, S., Sarkisyan, G., Fracasso, C., Martelli, G., Lacivita, E., Berardi, F., Perrone, R., 2010. LP-211 is a brain penetrant selective agonist for the serotonin 5-HT(7) receptor. Neurosci. Lett. 481, 12–16.
King, T., Vera-Portocarrero, L., Gutierrez, T., Vanderah, T.W., Dussor, G., Lai, J., Fields, H.L., Porreca, F., 2009. Unmasking the tonic-aversive state in neuropathic pain. Nat. Neurosci. 12, 1364–1366.
LaBuda, C.J., Fuchs, P.N., 2000. A behavioral test paradigm to measure the aversive quality of inflammatory and neuropathic pain in rats. Exp. Neurol. 163, 490–494.
LaGraize, S.C., Labuda, C.J., Rutledge, M.A., Jackson, R.L., Fuchs, P.N., 2004. Differential effect of anterior cingulate cortex lesion on mechanical hypersensitivity and escape/avoidance behavior in an animal model of neuropathic pain. Exp. Neurol. 188, 139–148.
Leopoldo, M., Lacivita, E., De Giorgio, P., Fracasso, C., Guzzetti, S., Caccia, S., Contino, M., Colabufo, N.A., Berardi, F., Perrone, R., 2008. Structural modifications of *N*-(1,2,3,4-tetrahydronaphthalen-1-yl)-4-aryl-1-piperazinehexanamides: influence on lipophilicity and 5-HT(7) receptor activity. Part III. J. Med. Chem. 51, 5813–5822.
Li, X.Y., Ko, H.G., Chen, T., Descalzi, G., Koga, K., Wang, H., Kim, S.S., Shang, Y., Kwak, C., Park, S.W., Shim, J., Lee, K., Collingridge, G.L., Kaang, B.K., Zhuo, M., 2010. Alleviating neuropathic pain hypersensitivity by inhibiting PKMzeta in the anterior cingulate cortex. Science 330, 1400–1404.
Li, S.F., Zhang, Y.Y., Li, Y.Y., Wen, S., Xiao, Z., 2014. Antihyperalgesic effect of 5-HT7 receptor activation on the midbrain periaqueductal gray in a rat model of neuropathic pain. Pharmacol. Biochem. Behav. 127, 49–55.
Lin, H., Heo, B.H., Kim, W.M., Kim, Y.C., Yoon, M.H., 2015. Antiallodynic effect of tianeptine via modulation of the 5-HT7 receptor of GABAergic interneurons in the spinal cord of neuropathic rats. Neurosci. Lett. 598, 91–95.
Nativio, P., Zoratto, F., Romano, E., Lacivita, E., Leopoldo, M., Pascale, E., Passarelli, F., Laviola, G., Adriani, W., 2015. Stimulation of 5-HT7 receptor during adolescence determines its persistent upregulation in adult rat forebrain areas. Synapse 69, 533–542.
Navratilova, E., Porreca, F., 2014. Reward and motivation in pain and pain relief. Nat. Neurosci. 17, 1304–1312.
Nolan, M.F., Dudman, J.T., Dodson, P.D., Santoro, B., 2007. HCN1 channels control resting and active integrative properties of stellate cells from layer II of the entorhinal cortex. J. Neurosci. 27, 12440–12451.
Perez-Garci, E., Larkum, M.E., Nevian, T., 2013. Inhibition of dendritic Ca2+ spikes by GABAB receptors in cortical pyramidal neurons is mediated by a direct Gi/o-beta-subunit interaction with Cav1 channels. J. Physiol. 591, 1599–1612.
Postea, O., Biel, M., 2011. Exploring HCN channels as novel drug targets. Nat. Rev. Drug Discov. 10, 903–914.
Qu, C., King, T., Okun, A., Lai, J., Fields, H.L., Porreca, F., 2011. Lesion of the rostral anterior cingulate cortex eliminates the aversiveness of spontaneous neuropathic pain following partial or complete axotomy. Pain 152, 1641–1648.
Ruocco, L.A., Treno, C., Gironi Carnevale, U.A., Arra, C., Boatto, G., Nieddu, M., Pagano, C., Illiano, P., Barbato, F., Tino, A., Carboni, E., Laviola, G., Lacivita, E., Leopoldo, M., Adriani, W., Sadile, A.G., 2014. Prepuberal stimulation of 5-HT7-R by LP-211 in a rat model of hyper-activity and attention-deficit: permanent effects on attention, brain amino acids and synaptic markers in the fronto-striatal interface. PLoS One 9, e83003.
Santello, M., Nevian, T., 2015. Dysfunction of cortical dendritic integration in neuropathic pain reversed by serotoninergic neuromodulation. Neuron 86, 233–246.
Santoro, B., Piskorowski, R.A., Pian, P., Hu, L., Liu, H., Siegelbaum, S.A., 2009. TRIP8b splice variants form a family of auxiliary subunits that regulate gating and trafficking of HCN channels in the brain. Neuron 62, 802–813.
Sieber, A.R., Min, R., Nevian, T., 2013. Non-Hebbian long-term potentiation of inhibitory synapses in the thalamus. J. Neurosci. 33, 15675–15685.
Simons, L.E., Elman, I., Borsook, D., 2014. Psychological processing in chronic pain: a neural systems approach. Neurosci. Biobehav. Rev. 39, 61–78.
Slassi, A., Isaac, M., Xin, T., 2004. Recent progress in 5-HT7 receptors: Potential treatment of central and peripheral nervous system diseases. 14 pp. 1009–1027.
Tang, Z.Q., Trussell, L.O., 2015. Serotonergic regulation of excitability of principal cells of the dorsal cochlear nucleus. J. Neurosci. 35, 4540–4551.
Yesilyurt, O., Seyrek, M., Tasdemir, S., Kahraman, S., Deveci, M.S., Karakus, E., Halici, Z., Dogrul, A., 2015. The critical role of spinal 5-HT7 receptors in opioid and non-opioid type stress-induced analgesia. Eur. J. Pharmacol. 762, 402–410.
Zhuo, M., 2008. Cortical excitation and chronic pain. Trends Neurosci. 31, 199–207.
Zhuo, M., 2016. Neural mechanisms underlying anxiety-chronic pain interactions. Trends Neurosci. 39, 136–145.